Journal of Controlled Release 347 (2022) 500–507

Contents lists available at ScienceDirect

Journal of Controlled Release

journal homepage: www.elsevier.com/locate/jconrel

Dose-response assessment of cerebral P-glycoprotein inhibition *in vivo* with [^{18}F]MC225 and PET

Lara Garcia-Varela [a,b,1], Pascalle Mossel [a,1], Pablo Aguiar [b], Daniel A. Vazquez-Matias [a], Aren van Waarde [a], Antoon T.M. Willemsen [a], Anna L. Bartels [c], Nicola A. Colabufo [d], Rudi A.J.O. Dierckx [a], Philip H. Elsinga [a], Gert Luurtsema [a,*]

[a] Department of Nuclear Medicine and Molecular Imaging, University of Groningen, University Medical Center Groningen, Hanzeplein 1, P.O. Box 30001, 9713 GZ Groningen, the Netherlands
[b] Department of Nuclear Medicine and Molecular Imaging Group, Clinical University Hospital, IDIS Health Research Institute, s/n A, Travesía da Choupana, 15706 Santiago de Compostela, Spain
[c] Department of Neurology, Ommelander Ziekenhuis Groningen, Pastorieweg 1, 9679 BJ, Scheemda, the Netherlands.
[d] Dipartimento di Farmacia-Scienze del Farmaco, Università degli Studi di Bari "A. Moro", via Orabona, 4, 70125 Bari, Italy

ARTICLE INFO

Keywords:
Dosing
Drug action
Efflux transporters
P-glycoprotein
Pharmacokinetics
Radiotracer sensitivity

ABSTRACT

The Blood-Brain Barrier P-glycoprotein (P-gp) function can be altered in several neurodegenerative diseases and due to the administration of different drugs which may cause alterations in drug concentrations and consequently lead to a reduced effectiveness or increased side-effects. The novel PET radiotracer [^{18}F]MC225 is a weak P-gp substrate that may show higher sensitivity to detect small changes in P-gp function than previously developed radiotracers. This study explores the sensitivity of [^{18}F]MC225 to measure the dose-dependent effect of P-gp inhibitor tariquidar. Twenty-three rats were intravenously injected with different doses of tariquidar ranging from 0.75 to 12 mg/kg, 30-min before the dynamic [^{18}F]MC225-PET acquisition with arterial sampling. Tissue and blood data were fitted to a 1-Tissue-Compartment-Model to obtain influx constant K_1 and distribution volume V_T, which allow the estimation of P-gp function. ANOVA and post-hoc analyses of K_1 values showed significant differences between controls and groups with tariquidar doses >3 mg/kg; while applying V_T the analyses showed significant differences between controls and groups with tariquidar doses >6 mg/kg. Dose-response curves were fitted using different models. The four-parameter logistic sigmoidal curve provided the best fit for K_1 and V_T data. Half-maximal inhibitory doses (ID_{50}) were 2.23 mg/kg (95%CI: 1.669–2.783) and 2.93 mg/kg (95%CI: 1.135–3.651), calculated with K_1 or V_T values respectively. According to the dose-response fit, differences in [^{18}F]MC225-K_1 values could be detected at tariquidar doses ranging from 1.37 to 3.25 mg/kg. Our findings showed that small changes in the P-gp function, caused by low doses of tariquidar, could be detected by [^{18}F]MC225-K_1 values, which confirms the high sensitivity of the radiotracer. The results suggest that [^{18}F]MC225 may allow the quantification of moderate P-gp impairments, which may allow the detection of P-gp dysfunctions at the early stages of a disease and potential transporter-mediated drug-drug interactions.

1. Introduction

P-glycoprotein (P-gp) is an efflux transporter that belongs to the ATP-Binding Cassette (ABC) transporter family and is coded by the ABCB1 gene in humans and Abcb1a and Abcb1b genes in rodents. In the brain, P-gp is located at the luminal side of the endothelial cells and its main function is to protect the Central Nervous System (CNS) from neurotoxic compounds. P-gp pumps a wide variety of substances from the brain back to the blood, and thereby, contributes to the maintenance of homeostasis in the CNS [1–3].

P-gp has gained special attention since dysfunctions of this transporter have been described in several CNS pathologies. Patients with Alzheimer's (AD) or Parkinson's Disease (PD) have shown a decrease in the P-gp function [4]. Recent research suggested that one of the main

* Corresponding author.
E-mail address: g.luurtsema@umcg.nl (G. Luurtsema).
[1] Lara Garcia-Varela and Pascalle Mossel have contributed equally to the work and share the first authorship.

https://doi.org/10.1016/j.jconrel.2022.05.026
Received 18 January 2022; Received in revised form 9 May 2022; Accepted 11 May 2022
Available online 20 May 2022

characteristics of AD: the accumulation of amyloid-β inside the brain, may be related to this decrease in P-gp function since amyloid-β is a P-gp substrate [5,6]. Moreover, alterations in P-gp function can modify the effectiveness and toxicity of CNS drugs [7,8]. Upregulation of P-gp function has been associated with drug resistance since the increase in function does not reduce the entry of neurotoxic compounds in the brain but also the entry of chemotherapeutics, antibiotics, antidepressants, and antiepileptic drugs [9–11]. For instance, patients with intractable epilepsy, that do not adequately respond to medication, show increased P-gp expression and function in the epileptogenic focus [12]. On the contrary, a decrease in P-gp function may increase the side effects and toxicity of CNS drugs by limiting their efflux from the brain.

Since the P-gp transporter is implied in several brain disorders and transporter-mediated drug-drug interactions (DDIs), it is of interest to monitor its function at the Blood-Brain Barrier (BBB). Nowadays, the Food and Drug Administration (FDA) and the European Medicines Agency (EMA) recommend the performance of clinical drug interaction studies in cases where the investigational drug is suspected to be a transporter modulator. Such studies may be performed using a transporter substrate of which the pharmacokinetic profile is altered after coadministration of a transporter modulator [13–15]. Molecular imaging techniques that allow the assessment of biological processes *in vivo* such as Positron Emission Tomography (PET) are appropriate measurement tools to evaluate P-gp function at the BBB *in vivo*. PET determines the tissue distribution of radiolabeled compounds (radiotracers) that are intravenously injected before the acquisition of the PET image [16]. To assess the P-gp function by PET imaging, a radiolabeled P-gp substrate is used whose distribution can be altered by the coadministration of P-gp modulators which would provide information about the transporter function.

The most used PET radiotracer for monitoring the P-gp function is (*R*)-[^{11}C]verapamil, however, this radiotracer has some drawbacks that limit its use [17]. (*R*)-[^{11}C]verapamil is an avid substrate of P-gp (showing high affinity for the transporter) and therefore, at baseline conditions, when the efflux pump is working properly, the accumulation of (*R*)-[^{11}C]verapamil inside the brain is neglectable [17]. Thus, (*R*)-[^{11}C]verapamil can detect decreases in P-gp function which cause an increase in radiotracer uptake [18], but (*R*)-[^{11}C]verapamil cannot demonstrate increases in the P-gp function, since decreases of the already low baseline radiotracer accumulation in the brain are undetectable. This very low baseline uptake also hampers the fusion and registration of functional PET images with anatomic images (CT or MRI) [19]. In addition, (*R*)-[^{11}C]verapamil may have limited sensitivity to detect small changes in the P-gp function. A study performed in heterozygous (Abcb1/b $^{(+/-)}$) and homozygous (Abcb1/b $^{(-/-)}$) knockout mice found that the brain uptake of (*R*)-[^{11}C]verapamil did not significantly change when the P-gp expression levels were reduced by 50%. However, the brain uptake of the radiotracer was increased in the homozygous mice (which completely lacked P-gp). The conclusion of this study was that avid substrates as (*R*)-[^{11}C]verapamil can only detect large changes (>50%) in BBB P-gp function [20].

(*R*)-[^{11}C]verapamil was shown to be useful in detecting changes in the P-gp function both after the administration of a high dose of a P-gp inhibitor and in completely P-gp knockout mice [21]. However, when pathophysiological changes in P-gp function were monitored with (*R*)-[^{11}C]verapamil, discrepant outcomes were reached which may be due to the fact that verapamil is a strong substrate of P-gp. As an example, in one study no significant changes of (*R*)-[^{11}C]verapamil uptake were found in early-stage PD patients compared to healthy volunteers [22]. However, an earlier study reported a significant increase of (*R*)-[^{11}C]verapamil uptake in PD patients, although this increase was limited to the midbrain [23]. A significant increase in the brain uptake of (*R*)-[^{11}C]verapamil was observed in patients with AD compared to healthy age-matched controls which suggested a decreased P-gp function in AD. However, this study did not find significant differences in the K_1 values of the radiotracer [24], which is considered the best kinetic parameter to measure the P-gp function [25,26]. Also, a PET study did not find significant differences between young and elderly subjects in the global uptake of (*R*)-[^{11}C]verapamil in the CNS [27], whereas several post-mortem studies reported decreased P-gp expression in aging [5,28]. (*R*)-[^{11}C]verapamil was also used to study the P-gp function in patients with temporal lobe epilepsy. Although such patients are believed to have an increased P-gp function and expression [29], the authors did not detect significant differences in (*R*)-[^{11}C]verapamil uptake between the epileptogenic focus and the contralateral area of the brain [30].

To overcome the low baseline uptake and improve the limited sensitivity of avid P-gp substrates in PET imaging, research is focused on the development of radiolabeled substrates with weaker affinity for P-gp, such as [^{11}C]metoclopramide and [^{18}F]MC225. These radiotracers show higher uptake values inside the brain at baseline conditions compared with (*R*)-[^{11}C]verapamil [31,32]. The kinetics of these radiotracers have already been evaluated in different animal species and in humans, and these allow measurement of both decreases and increases of the P-gp function at the BBB [33–37]. It has been suggested that the higher baseline uptake of these radiotracers may also allow the detection of small changes in the P-gp function with higher sensitivity than (*R*)-[^{11}C]verapamil. For avid substrates, there is extremely low uptake in the brain not only at baseline but even after partial P-gp blocking, because the transporter pumps the radiotracer very efficiently out of the brain, limiting the range in which alterations of P-gp function can be measured. Thus, a somewhat reduced affinity of a PET tracer for P-gp may enhance the assessment of the functionality of the transporter in brain disorders and the detection of transporter-mediated DDIs.

This study aims to explore the sensitivity of the novel radiotracer [^{18}F]MC225 to measure gradual changes in the P-gp function. To this aim, we performed an *in vivo* dose-response evaluation of tariquidar on the BBB P-gp function, using [^{18}F]MC225-PET. The results were compared to dose-response data of (*R*)-[^{11}C]verapamil reported in previous publications.

2. Material and methods

2.1. Chemicals

Tariquidar was purchased from ToCris (Bio-Techne Ltd., Abingdon, United Kingdom). For intravenous injection, tariquidar was dissolved in a vehicle solution composed of 5% Dimethyl Sulfoxide (DMSO), 10% of TWEEN 20, 25% of polyethylene glycol 400 (PEG400), and 65% of H_2O, in a total volume of 0.9 ml as has been previously described [32].

2.2. Radiosynthesis

The production and quality control procedures of [^{18}F]MC225 were performed as previously described [32,38].

2.3. Animals

All the experiments were approved by the Institutional Animal Care and Use Committee of the University of Groningen and were performed in accordance with the Animal Welfare Act of the European Communities Council Directive. The protocol of the study was approved by the National Committee on Animal Experiments of the Netherlands and the Institutional Animal Care and Use Committee of the University of Groningen (CCD license: AVD 105020198648, IvD protocol: 198648–01-003). Twenty-three adult male outbred Wistar rats (RjHan: WI) (body-weight at delivery 230–260 g) were obtained from Janvier Labs (France). Exclusively male rats were selected, in order to avoid influence of the estrogen cycle on P-gp function at the BBB and because gender differences in the biodistribution of P-gp radiotracers have been found in humans [39] The animals were acclimatized at the Central Animal Facility of the University Medical Center Groningen for at least 7 days before starting the experiment. They were housed in groups of two or

three animals per cage in a room with controlled temperature and humidity. Food and water were available *ad libitum*.

Rats were randomly divided into seven groups which were injected with different doses of the P-gp inhibitor tariquidar, ranging from 0.75 mg/kg to 12 mg/kg (Table 1). Controls (group 1) received only the vehicle solution. The administration of either vehicle or treatment in vehicle was performed under isoflurane anesthesia through a tail vein 30 min before the PET scan since according to the literature the maximum effect of tariquidar in rats occurs 30 min after injection [32,40]. Supplemental Table 1 shows different doses of tariquidar in each group.

2.4. PET imaging

Firstly, animals (320 ± 23 g) were anesthetized using an induction dose of 5% isoflurane in 95% oxygen, and during the study, the anesthesia was maintained at 1.5–2% isoflurane. Next, a cannula was placed in the femoral artery to obtain arterial blood samples during the scan. Then, the anesthetized animals were positioned in the microPET camera (microPET Focus 220, Siemens Medical Solutions, Malvern, PA, USA) and injected with tariquidar or the vehicle solution *via* the tail vein. A transmission scan was performed for 10 min using a ^{57}Co point source, in order to correct the subsequently acquired dynamic PET data for attenuation and scatter. Thirty minutes after the administration of tariquidar or vehicle, a 60-min-dynamic PET scan was started simultaneously with injection of the radiotracer. [^{18}F]MC225 (average dose 21.61 ± 4.45 MBq) was administered during a period of 1 min using an infusion pump. The heart rate and oxygen saturation of the animals were monitored during the PET scan, using pulse oximeters, and their body temperature was maintained close to the physiological value using heating pads.

2.5. Blood and metabolite analysis

Arterial blood samples (0.1 ml) were collected every ten seconds during the first minute and at 1.5, 2, 3, 5, 7.5, 10, 15, 30, 45, and 60 min after the start of the scan. The amount of drawn blood was replaced by saline solution (0.9% NaCl with heparin 1%). Blood samples were used to determine radioactivity in whole-blood and plasma as previously described [41]. Radioactive metabolites were analyzed using plasma samples at 10 s, 1, 3, 5, 7.5, 10, 15, 30, 45, and 60 min using thin-layer chromatography (TLC) as described elsewhere [41].

Time-activity curves (TAC) of the whole-blood and plasma were corrected by the dose injected (ID) and the bodyweight (BW) of the animal and expressed as Standardized Uptake Values (SUV) *versus* time. SUV is a semiquantitative parameter that is used for normalization of radioactivity outcomes.

$$SUV(t) = \frac{Radioactivity\ concentration\ in\ blood\ or\ plasma\ samples\ (t)}{ID/BW}$$

The SUV-TAC of plasma corrected for metabolites was calculated by multiplying the plasma SUV values by the time-dependent parent fraction of the radiotracer in plasma. The SUV metabolite-corrected plasma and SUV whole-blood TACs were used as input function for pharmacokinetic modeling since it represents the amount of radiotracer available to enter the cells.

Table 1
[^{18}F]MC225 V_T and K_1 values (mean ± SD) in the whole-brain calculated using 1TCM after the administration of different doses of tariquidar.

Groups	Number of animals (n)	V_T	K_1 (mL/mL/min)
Control	3	7.44 ± 0.51	0.25 ± 0.03
Dose Tariquidar			
0.75 mg/kg	4	6.56 ± 1.45	0.26 ± 0.07
1.5 mg/kg	4	8.11 ± 2.34	0.39 ± 0.14
3.0 mg/kg	3	15.13 ± 3.74	0.82 ± 0.16*
6.0 mg/kg	3	18.89 ± 5.33*	1.07 ± 0.13*
8.0 mg/kg	3	17.59 ± 3.54*	0.96 ± 0.21*
12 mg/kg	3	16.36 ± 1.72*	0.95 ± 0.06*

* Significantly different compared to the control group ($p < 0.05$)

2.6. Reconstructions and data-analysis

The emission scan data were reconstructed in the following 21 frames: 6 × 10 s, 4 × 30 s, 2 × 60 s, 1 × 120 s, 1 × 180 s, 4 × 300 s, and 3 × 600 s, using OSEM 2D, 4 iterations, and 16 subsets. Emission sinograms were corrected for decay and data from transmission scans were used for attenuation and scatter corrections.

PET images were analyzed using PMOD v3.5 software (PMOD Technologies, Zurich, Switzerland). PET images were co-registered with an [^{18}F]MC225 specific brain template [41,42] using rigid matching. Predefined brain regions were selected as volumes of interest (VOI) [41] and tissue radioactivity (Bq/mL) was calculated to generate tissue-TACs (TACs). Radioactivity in whole-blood samples and metabolite corrected plasma samples was used as input for the kinetic modeling. Since previous studies suggested the 1-Tissue Compartment Model (1TCM) as the model of choice to fit [^{18}F]MC225 data in rats [32], this model was used to calculate the volume of distribution (V_T) as well as the influx constant K_1. In compartment models, V_T refers to the ratio of the radiotracer concentrations in target tissue and plasma at equilibrium. K_1 represents the unidirectional transport of the radiotracer from the plasma to the first tissue compartment. K_1 depends on the blood flow and the capillary permeability surface area product. Since SUV can be calculated more easily, tissue SUV-TACs were also generated by correcting the tissue radioactivity of each VOI for the dose injected and the bodyweight of the animal. Moreover, $SUV_{50–60}$ was calculated using the last frame of the scan (50 to 60 min after radiotracer injection) and maximum SUV values of the whole-brain SUV-TACs were also calculated (SUV_{max}).

2.7. Parametric images

Parametric maps of a representative animal of each group were generated using a basic function 1-TCM and the metabolite-corrected plasma TAC as input function. Parametric images show K_1 values of the brain in all experimental groups.

2.8. Statistics

Descriptive data are presented as mean ± standard deviation unless otherwise mentioned. IBM SPSS Statistics 23 software (Armonk, New York, USA) was used for the statistical analysis. Differences among groups were analyzed using one-way ANOVA with post-hoc Tukey HSD. A p-value of <0.05 was considered statistically significant.

Kinetic constants obtained from the 1TCM (K_1 and V_T) with their corresponding standard errors (SE%) were plotted against the different tariquidar doses and several dose-response curves were fitted to these data using MATLAB (The MathWorks, Inc). A weighting factor based on the standard errors of the obtained K_1 and V_T values was applied to the dose-response fit. The fits were used to determine the half-maximal inhibitory dose (ID_{50}) of tariquidar, the bottom and top values of K_1 or V_T, as well as the 95% Confidence Intervals (95%CI) of these parameters.

3. Results

3.1. Radiosynthesis

The radiotracer [^{18}F]MC225 was produced in 95 ± 8 min using a two-step synthesis with a total radiochemical yield of 7.8 ± 1.1% (decay-corrected from the end of bombardment of [^{18}F]F$^-$). The molar activity of the radiotracer was higher than 200 TBq/mmol and the radiochemical purity was 97.2 ± 0.7%.

3.2. Pharmacokinetics

The V_T and K_1, values at different tariquidar doses are shown in Table 1. Increases in tariquidar dose caused a gradual increase in K_1 and V_T values until the dose of 6 mg/kg where they reached a plateau. The K_1 increased from 0.25 ± 0.03 in the control group to a maximum of 1.07 ± 0.13 caused by a 6 mg/kg dose of tariquidar ($p < 0.001$) (Fig. 1). A significant increase in K_1 values with respect to the control group was already observed at a dose of 3 mg/kg, where the K_1 value was 0.82 ± 0.16 ($p = 0.001$). V_T increased from 7.44 ± 0.51 in the control group to a maximum of 18.89 ± 5.33 at a tariquidar dose of 6 mg/kg ($p = 0.003$).

3.3. Dose-response fitting curve

Different dose-response curves were fitted to the K_1 and V_T data: the hyperbola or saturation binding curve, the symmetrical sigmoidal curve and the symmetrical sigmoidal curve with variable slope also called four-parameter logistic sigmoidal curve (4PL). The best fits were selected according to the sum of square estimate errors (SSE), the R-square and the adjusted R-square. The results showed that the most adequate curve to fit the data was the 4PL sigmoidal curve (Table 2): Y (x) = Bottom+(Top-Bottom)/(1 + 10^((C-x)*HillSlope)), Y(x) being the V_T and K_1 values obtained with different doses of tariquidar, C represents the half-maximal inhibitory concentration (ID_{50}), X the dose of tariquidar and the HillSlope is a parameter that describes the steepness of the curve.

The 4PL sigmoidal curve fit using either K_1 or V_T values provided similar results (Table 2). Using the K_1 whole-brain values, the estimated ID_{50} was 2.226 (95%CI: 1.669–2.783) mg/kg and using the V_T values it was 2.393 (95%IC: 1.1135–3.651) mg/kg. The estimated bottom value of K_1 was 0.2342 (95%CI: 0.1078–0.3612) ml/ml/min and the bottom value of V_T was 6.978 (95%CI: 2.199–11.76). The estimated top value was 1.006 (95%CI: 0.9098–1.102) ml/ml/min for K_1 and 18.22 for V_T (95%CI: 16.23–20.21). According to this dose-response fit, a detectable range of tariquidar doses could be defined from 1.37 to 3.25 mg/kg using K_1 values, but not using V_T values. Fig. 2 shows the different dose-response curve fits for K_1 and V_T and Table 3 shows the bottom, top, ID_{50} and HillSlope values obtained with the 4PL curve.

3.4. SUV analysis

SUV-TACs of the whole-brain region can be observed in Supplemental Fig. 2. $SUV_{50–60min}$ values of the whole-brain region were calculated using the last frame of the dynamic PET scan (Fig. 4). Significant differences were found only between the control (0.42 ± 0.08) and the 6 mg/kg and 8 mg/kg groups (1.02 ± 0.07 and 1.25 ± 0.29, respectively) (Fig. 3). V_T and K_1 outcome parameters of the 1TCM were compared with the $SUV_{50–60}$ and moderate correlations were found for both K_1 (Adjusted $R^2 = 0.692$, $p < 0.001$) and V_T (Adjusted $R^2 = 0.664$, $p < 0.001$) (Supplemental Fig. 3). For SUV_{max} significant differences were found between the control group (0.80 ± 0.16) and the group treated with 8 mg/kg tariquidar (2.40 ± 0.33). Between SUV_{max} and K_1 and V_T also moderate correlations were present (Adjusted $R^2 = 0.629$, $p < 0.001$ and Adjusted $R^2 = 0.525$, $p < 0.001$, respectively) (Supplemental Fig. 3).

Table 2
Goodness of the fit of different dose-response curves fitted to the K_1 and V_T data.

Curve	Equation	Y-variable	Goodness of the fit		
			SEE	R-square	Adjusted R-square
Hyperbola	Y(x) = (Bmax*x)/(Kd + x)	K_1	1.238	0.7587	0.7472
		V_T	4610	0.471	0.4458
Symmetrical Sigmoidal	Y (x) = Bottom +(Top-Bottom)/ (1 + 10^((C-x)))	K_1	0.2875	0.8955	0.8851
		V_T	2706	0.6895	0.6584
4PL sigmoidal curve	Y (x) = Bottom+ (Top-Bottom)/ (1 + 10^((C-x) *HillSlope))	K_1	0.4866	0.9051	0.8902
		V_T	2705	0.6897	0.6407

4. Discussion

This study provides insight into the sensitivity of the novel PET radiotracer [^{18}F]MC225 to detect changes of P-gp function, using dose-dependent inhibition of P-gp function at the rodent BBB by tariquidar. [^{18}F]MC225 is a weak P-gp substrate and it is expected to show higher sensitivity to detect small changes in the P-gp function than avid P-gp substrates such as (*R*)-[^{11}C]verapamil. The current study also provides an overview of methods for [^{18}F]MC225 data analysis in situations where the P-gp function is partially blocked.

One important finding of this study is the gradual increase in K_1 and V_T values at higher doses of tariquidar until saturation is reached. Our results showed that [^{18}F]MC225 was able to detect small changes in the

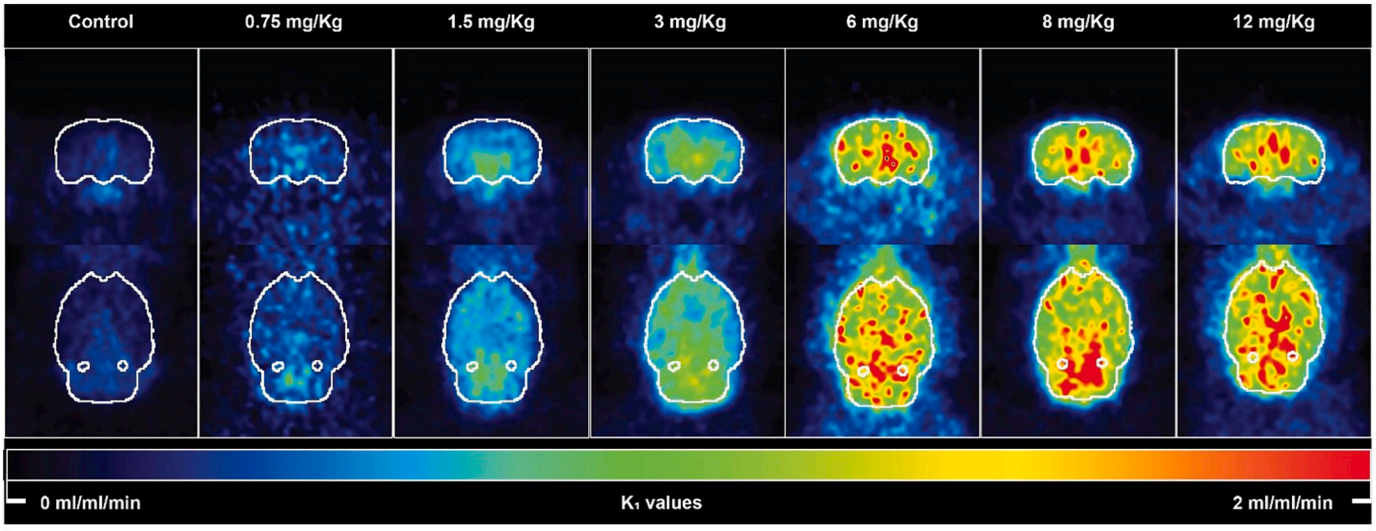

Fig. 1. K_1 parametric maps in transversal (images above) and frontal (images below) planes obtained with [^{18}F]MC225 of a representative subject of each experimental group.

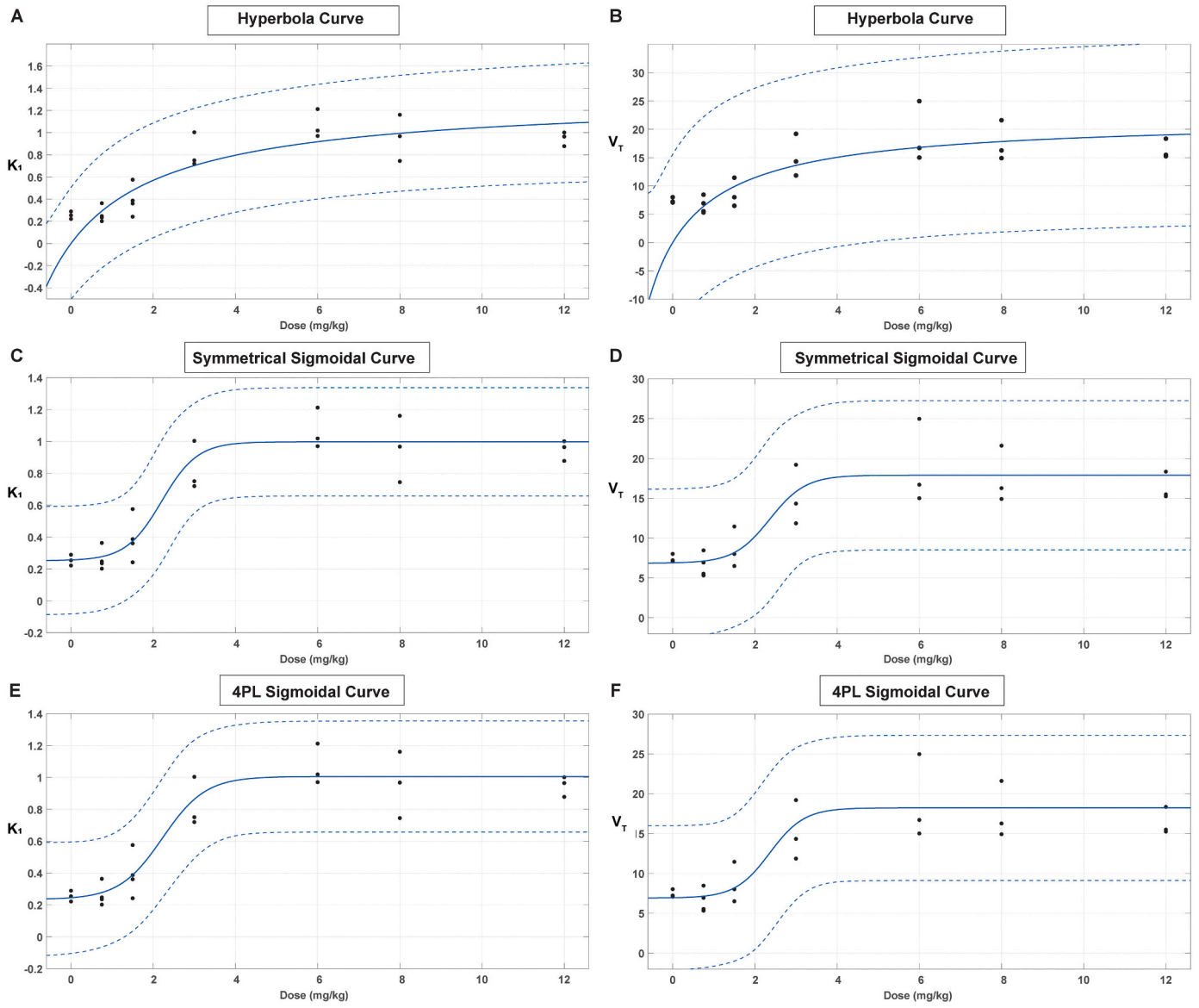

Fig. 2. Hyperbola (A and B), symmetrical sigmoidal (C and D) and 4PL sigmoidal curve (E and F) fits for the whole-brain K_1 and V_T values in response to different doses of tariquidar.

Table 3
Nonlinear fit results of the 4PL sigmoidal curve to K_1 and V_T data for whole-brain.

Fitting curve	Response			
Symmetrical Sigmoidal Variable Slope	K_1 (ml/ml/min)	95%CI	V_T	95%CI
Bottom	0.2342	(0.1072–0.3612)	6.978	(2.199–11.76)
Top	1.006	(0.9098–1.102)	18.22	(16.23–20.21)
ID_{50} (mg/kg)	2.226	(1.669–2.783)	2.393	(1.135–3.651)
HillSlope	0.8305	(0.2439–1.417)	0.9163	(−0.6082–2.441)

P-gp function caused by low doses of tariquidar. Thus, a detectable range of tariquidar doses could be defined: doses as small as 1.37 mg/kg to 3.25 mg/kg (with ID_{50} of 2.226 mg/kg) using [^{18}F]MC225 K_1 values. The ability to detect these small changes may have a great clinical value since it opens the possibility to evaluate moderate P-gp function impairments caused by a disease or by the administration of a P-gp modulator. Such impairments can affect the distribution of pharmaceuticals that are P-gp substrates, as their uptake in the CNS is inversely correlated with the P-gp function [7]. Even small changes in P-gp function might cause a gradual increase in the bioavailability of these drugs, similar to the increases we found in the brain uptake of [^{18}F]MC225. Moreover, this study confirmed the higher V_T and K_1 values of [^{18}F]MC225 at baseline and in the presence of low doses of tariquidar, as compared with the corresponding values of (*R*)-[^{11}C]verapamil from previous studies. A V_T of 7.44 ± 0.5 was found in control animals, compared with a baseline V_T of 1.27 ± 0.15 for (*R*)-[^{11}C]verapamil [40]. Also, the K_1 values of [^{18}F]MC225 at baseline were higher than those of (*R*)-[^{11}C]verapamil, (0.25 ± 0.03 *vs* 0.016 ± 0.05, respectively). These higher uptake values of [^{18}F]MC225 allow the measurement of both decreases and increases in the P-gp function [32,36] and broaden the range of P-gp measurements. Since increases in P-gp function are related to resistance to several drugs that are P-gp substrates, [^{18}F]MC225 PET may be an important tool in the drug development process for the screening of P-gp interactions of novel CNS candidates.

Dose-response curve fitting (4PL curve) provided an ID_{50} value of 2.18 ± 0.27 for P-gp inhibition with tariquidar using [^{18}F]MC225 and the K_1 values of the study groups. This ID_{50} value is slightly lower than

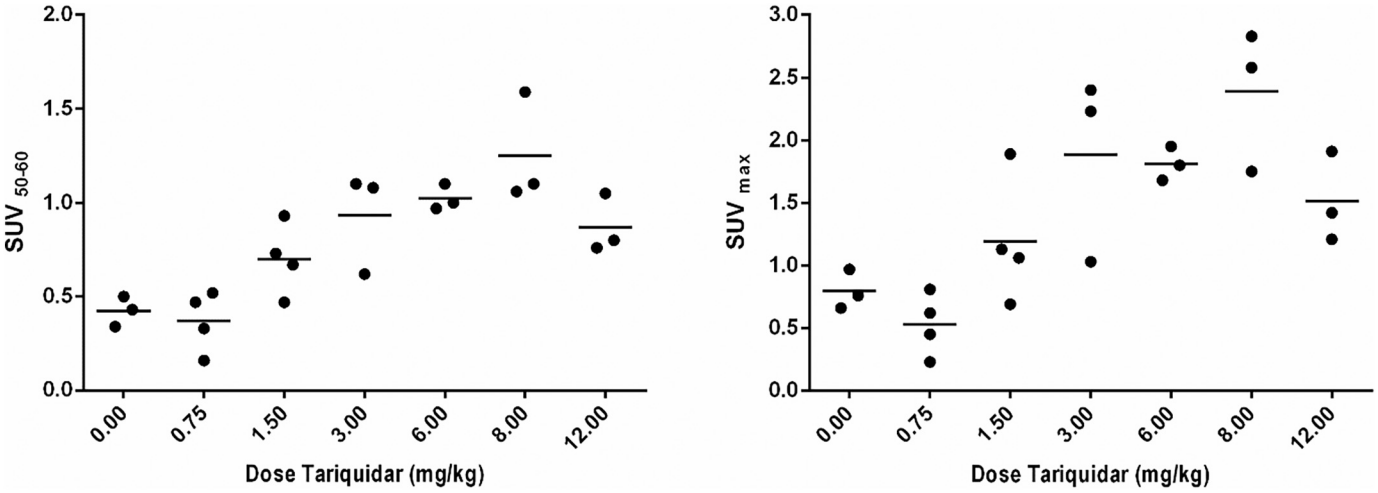

Fig. 3. $SUV_{50–60}$ (A) and SUV_{max} (B) values of the subjects treated with different doses of tariquidar. The solid line represents the mean of each group.

the one calculated by Kuntner et al. using (*R*)-[^{11}C]verapamil (ID_{50} = 3.00 ± 0.19 mg/kg). The 4PL sigmoidal curve provided K_1 and V_T top values of 1.06 and 18.22 respectively, which were both reached at a dose of 6 mg/kg of tariquidar. Similar maximum values were achieved with (*R*)-[^{11}C]verapamil at a similar dose of tariquidar [40]. According to the dose-response fit, doses between 1.37 mg/kg and 3.24 mg/kg may cause an increase in the K_1 values of [^{18}F]MC225 and doses between 2.25 and 3.12 mg/kg may cause a detectable increase in the V_T values of [^{18}F]MC225. Therefore, both the statistical analysis and the dose-response fit highlight the K_1 as a more sensitive parameter to detect small changes in the P-gp function with [^{18}F]MC225. These findings are in line with previous publications in which K_1 was shown to be the parameter of choice to study BBB P-gp function with [^{18}F]MC225 in both rodents and non-human primates [19,41].

Since kinetic modeling is a complicated and time-consuming form of analysis due to the requirement of arterial blood sampling, simplified methods for quantifying the P-gp function such as SUV measurements are preferred. For this reason, SUV values were also analyzed in the present study. However, the statistical analysis only showed significant differences between the $SUV_{50–60min}$ values of the control group and the groups treated with 6 and 8 mg/kg of tariquidar. In the case of SUV_{max}, the statistical analysis only revealed significant differences between the control group and the group treated with 8 mg/kg. Comparison of Figs. 1 and 4 showed the lack of sensitivity of $SUV_{50–60min}$ to detect small increases in the [^{18}F]MC225 brain uptake. Therefore, this study emphasizes the use of kinetic modeling to estimate K_1 which may be the most adequate parameter to evaluate the P-gp function due to its sensitivity to detect changes in the P-gp function at low doses of tariquidar.

Wanek et al. studied the effect of tariquidar on the P-gp function in homozygous (Abcb1a/1b$^{(-/-)}$) and heterozygous (Abcb1a/1b$^{(+/-)}$) mice using (*R*)-[^{11}C]verapamil and PET [43]. In homozygous mice, the (*R*)-[^{11}C]verapamil brain uptake was significantly increased (3.9-fold) compared to controls. However, in heterozygous mice with a 50% reduction of P-gp expression at the BBB, the uptake of (*R*)-[^{11}C]verapamil was only minimally and not significantly increased [43]. Therefore, the authors concluded that (*R*)-[^{11}C]verapamil may not be able to detect small variations in the P-gp function (<50%) since this radiotracer is very effectively transported by P-gp [20,40]. In the same study, the brain distribution of (*R*)-[^{11}C]verapamil was evaluated in wild-type mice treated either with vehicle or escalating tariquidar doses, and a dose of 15 mg/kg of tariquidar was found to cause a similar (*R*)-[^{11}C]verapamil brain uptake as was observed in homozygous P-gp knockout

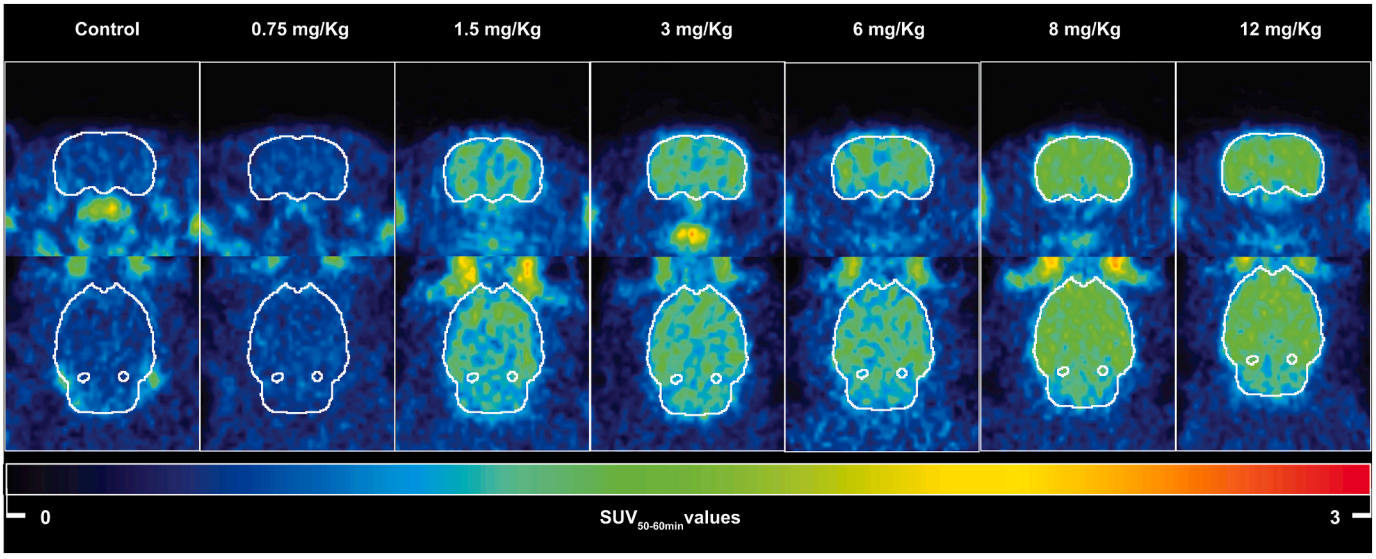

Fig. 4. SUV images in transversal (images above) and frontal (images below) planes calculated using the last frame of the dynamic PET (50 to 60 min after radiotracer injection) of a representative subject of each experimental group.

mice and a dose of 3 mg/kg of tariquidar a similar (*R*)-[^{11}C]verapamil brain uptake as in the heterozygous mice. Also, no significant differences in brain uptake of the radiotracer were observed between animals treated with vehicle and animals treated with 3 mg/kg of tariquidar. However, in our study, a significant increase in the K_1 compared to controls was already detected after the administration of 3 mg/kg and according to the 4PL sigmoidal curve fit, a trend towards increase could be already observed at a dose of 1.37 mg/kg tariquidar. Thus, these results suggest that [^{18}F]MC225 may be a more adequate radiotracer to detect moderate changes in the P-gp function than (*R*)-[^{11}C]verapamil.

A recent study also evaluated the sensitivity of [^{11}C]metoclopramide, another weak P-gp substrate PET radiotracer, to detect moderate changes in the P-gp function, however, the effect of the P-gp inhibition was measured using SUV measurements, instead of kinetic parameters obtained from pharmacokinetic analysis of the data [44]. Therefore, the data should be compared with caution since SUV measurements of the brain do not account for radio-metabolites which may interfere with the quantification. The authors found that the ID_{50} of tariquidar to increase [^{11}C]metoclopramide uptake was 1 mg/kg (95%CI: 0.78–1.5 mg/kg) and complete inhibition of the P-gp function was reached at a dose of 2 mg/kg. In our study, the ID_{50} was higher (2.18 ± 0.27 mg/kg of tariquidar) and complete inhibition of the P-gp function was observed at a dose of 6 mg/kg. Thus, [^{18}F]MC225 may detect decreases of P-gp function in a broader range of inhibitor concentrations than [^{11}C]metoclopramide. However, because of the methodological differences between published studies, a direct head-to-head comparison of [^{11}C]metoclopramide and [^{18}F]MC225 should be performed.

Dose-dependent effects of tariquidar on the metabolite-corrected plasma SUV-TAC of [^{18}F]MC225 were not observed and tariquidar did not affect the metabolism of the radiotracer, since no significant differences in the percentage of parent radiotracer were found among the groups (more information is provided in the Supplemental Data file).

According to the results of the dose-response fit, a saturation of the P-gp transporter function could be already observed with [^{18}F]MC225 after doses greater than 3.25 mg/kg of tariquidar, however, this may be related to the *a priori* selection of tariquidar doses evaluated in this study. The range of doses jumped from 3 to 6 mg/kg of tariquidar which could interfere in the dose-response fit, perhaps, an intermediate dose should have been included in this study. Further research should be undertaken to determine more precisely the range of doses that cause a detectable change in the [^{18}F]MC225 uptake.

One important limitation of the current study is that no head-to-head comparison between [^{11}C]MC225, (*R*)-[^{11}C]verapamil and [^{11}C]metoclopramide was performed. The comparison of the kinetics of [^{18}F]MC225 with those of (*R*)-[^{11}C]verapamil and [^{11}C]metoclopramide could only be done using literature data. Since scans were performed in different research centers and the data analysis methods were different, slight differences in study outcome could be expected. Although the same type of microPET scanner was used in our study and in the previous study by Kuntner et al. ((*R*)-[^{11}C]verapamil study), animals of the previous study were female rats whereas our study used male rats. This gender difference also complicates data comparison.

5. Conclusion

In the present study, we have validated the ability of [^{18}F]MC225 to measure gradual changes of the P-gp function at the BBB. Our results suggest that [^{18}F]MC225 may be capable of detecting small changes of P-gp function which may allow the quantification of moderate P-gp dysfunctions. The measurement of small alterations in the P-gp function could be of great value in drug development, as [^{18}F]MC225-PET scans may be able to identify pharmaceuticals that act as weak P-gp modulators. With this approach, [^{18}F]MC225 scans can contribute to the detection of transporter-mediated DDIs, and thereby, prevent drug resistance and toxicities caused due to the concomitant administration of drugs. Furthermore, [^{18}F]MC225 could be of great importance in the early diagnosis of neurodegenerative diseases, including Alzheimer's disease where the P-gp dysfunction can be the reason for amyloid-β accumulation. We suggest that [^{18}F]MC225 may allow the stratification of P-gp dysfunction in these diseases which may be useful for diagnosis and treatment selection.

Funding

GL received a research grant from Siemens Healthineers for appointing a PhD candidate.

Author contributions

Lara Garcia-Varela: Methodology, Software, Formal analysis, Investigation, Resources, Data Curation, Writing - Original Draft, Visualization. **Pascalle Mossel** Methodology, Software, Formal analysis, Investigation, Resources, Data Curation, Writing-Original Draft, Visualization. **Pablo Aguiar**: Software, Formal analysis, Writing - Review & Editing. **Daniel A. Vazquez-Matias**: Investigation, Resources. **Aren van Waarde**: Conceptualization, Methodology, Writing - Review & Editing. **Antoon T. M. Willemsen**: Formal analysis. **Anna L. Bartels**: Formal analysis, Writing - Review & Editing. **Nicola A. Colabufo**: Resources, Writing - Review & Editing. **Rudi A.J.O. Dierckx**: Writing - Review & Editing. **Philip H. Elsinga**: Writing - Review & Editing. **Gert Luurtsema**: Conceptualization, Methodology, Writing - Review & Editing, Supervision.

Declaration of Competing Interest

The other authors declare no competing interests.

Acknowledgments

The authors would like to thank Jürgen W.A. Sijbesma and Janine Doorduin for their assistance during the preclinical studies.

Appendix A. Supplementary data

Supplementary data to this article can be found online at https://doi.org/10.1016/j.jconrel.2022.05.026.

References

[1] J.H. Lin, M. Yamazaki, Role of P-glycoprotein in pharmacokinetics: clinical implications, Clin. Pharmacokinet. 42 (2003) 59–98, https://doi.org/10.2165/00003088-200342010-00003.
[2] W. Löscher, B. Gericke, Novel intrinsic mechanisms of active drug extrusion at the blood-brain barrier: potential targets for enhancing drug delivery to the brain? Pharmaceutics. 12 (2020) 966, https://doi.org/10.3390/pharmaceutics12100966.
[3] R. Bendayan, G. Lee, M. Bendayan, Functional expression and localization of P-glycoprotein at the blood brain barrier, Microsc. Res. Tech. 57 (2002) 365–380, https://doi.org/10.1002/jemt.10090.
[4] E. Gil-Martins, D.J. Barbosa, V. Silva, F. Remião, R. Silva, Dysfunction of ABC transporters at the blood-brain barrier: role in neurological disorders, Pharmacol. Ther. 213 (2020) 107554, https://doi.org/10.1016/j.pharmthera.2020.107554.
[5] S. Vogelgesang, I. Cascorbi, E. Schroeder, J. Pahnke, H.K. Kroemer, W. Siegmund, C. Kunert-Keil, L.C. Walker, R.W. Warzok, Deposition of Alzheimer's beta-amyloid is inversely correlated with P-glycoprotein expression in the brains of elderly non-demented humans, Pharmacogenetics. 12 (2002) 535–541, https://doi.org/10.1097/00008571-200210000-00005.
[6] F.C. Lam, R. Liu, P. Lu, A.B. Shapiro, J.-M. Renoir, F.J. Sharom, P.B. Reiner, β-Amyloid efflux mediated by p-glycoprotein, J. Neurochem. 76 (2001) 1121–1128, https://doi.org/10.1046/j.1471-4159.2001.00113.x.
[7] S.F. Zhou, Structure, Function and Regulation of P-Glycoprotein and its Clinical Relevance in Drug Disposition 38, 2008, pp. 802–832, https://doi.org/10.1080/00498250701867889.
[8] M. Lund, T.S. Petersen, K.P. Dalhoff, Clinical implications of P-Glycoprotein modulation in drug-drug interactions, Drugs 77 (2017) 859–883, https://doi.org/10.1007/s40265-017-0729-x.
[9] J.I. Fletcher, R.T. Williams, M.J. Henderson, M.D. Norris, M. Haber, ABC transporters as mediators of drug resistance and contributors to cancer cell biology, Drug Resist. Updat. 26 (2016) 1–9, https://doi.org/10.1016/j.drup.2016.03.001.

[10] M.M. Gottesman, T. Fojo, S.E. Bates, Multidrug resistance in cancer: role of ATP–dependent transporters, Nat. Rev. Cancer 2 (2002) 48–58, https://doi.org/10.1038/nrc706.

[11] W. Löscher, H. Potschka, Role of drug efflux transporters in the brain for drug disposition and treatment of brain diseases, Prog. Neurobiol. 76 (2005) 22–76, https://doi.org/10.1016/j.pneurobio.2005.04.006.

[12] G.-X. Wang, D.-W. Wang, Y. Liu, Y.-H. Ma, Intractable epilepsy and the P-glycoprotein hypothesis, Int. J. Neurosci. 126 (2016) 385–392, https://doi.org/10.3109/00207454.2015.1038710.

[13] Guideline on the Investigation of Drug Interactions, June 2012. (s. f.). http://www.ema.europa.eu/docs/en_GB/document_library/Scientific_guideline/2012/07/WC500129606.pdf, 2012.

[14] US Food and Drug Administration, In Vitro Drug Interaction Studies - Cytochrome P450 Enzyme and Transporter Mediated Drug Interactions, FDA Guid 1, 2020, pp. 1–46.

[15] US FDA, Guidance for Industry: Clinical Drug Interaction Studies —Cytochrome P450 Enzyme- and Transporter-Mediated Drug Interactions, https//www.fda.gov/media/134581/download. Accessed Oct. 18, 2020, 2020.

[16] O. Langer, Use of PET imaging to evaluate transporter-mediated drug-drug interactions, J. Clin. Pharmacol. (2016) S143–S156, https://doi.org/10.1002/jcph.722.

[17] G. Luurtsema, P. Elsinga, R. Dierckx, R. Boellaard, A. Waarde, PET tracers for imaging of ABC transporters at the blood-brain barrier: principles and strategies, Curr. Pharm. Des. 22 (2016) 5779–5785, https://doi.org/10.2174/1381612822666160810123634.

[18] J. Toyohara, Importance of P-gp PET imaging in pharmacology, Curr. Pharm. Des. 22 (2016) 5830–5836, https://doi.org/10.2174/1381612822666160804092258.

[19] L. García-Varela, D. Vállez García, P. Aguiar, T. Kakiuchi, H. Ohba, N. Harada, S. Nishiyama, T. Tago, P.H. Elsinga, H. Tsukada, N.A. Colabufo, R.A.J.O. Dierckx, A. van Waarde, J. Toyohara, R. Boellaard, G. Luurtsema, Head-to-head comparison of (R)-[11C]verapamil and [18F]MC225 in non-human primates, tracers for measuring P-glycoprotein function, Eur. J. Nucl. Med. Mol. Imaging (2021), https://doi.org/10.1007/s00259-021-05411-2.

[20] M. Bauer, N. Tournier, O. Langer, Imaging P-glycoprotein function at the blood–brain barrier as a determinant of the variability in response to central nervous system drugs, Clin. Pharmacol. Ther. 105 (2019) 1061–1064, https://doi.org/10.1002/cpt.1402.

[21] C.C. Wagner, M. Bauer, R. Karch, T. Feurstein, S. Kopp, P. Chiba, K. Kletter, W. Loscher, M. Muller, M. Zeitlinger, O. Langer, A pilot study to assess the efficacy of tariquidar to inhibit P-glycoprotein at the human blood-brain barrier with (R)-11C-verapamil and PET, J. Nucl. Med. 50 (2009) 1954–1961, https://doi.org/10.2967/jnumed.109.063289.

[22] A.L. Bartels, B.N.M. van Berckel, M. Lubberink, G. Luurtsema, A.A. Lammertsma, K.L. Leenders, Blood-brain barrier P-glycoprotein function is not impaired in early Parkinson's disease, Parkinsonism Relat. Disord. (2008), https://doi.org/10.1016/j.parkreldis.2007.11.007.

[23] R. Kortekaas, K.L. Leenders, J.C.H. Van Oostrom, W. Vaalburg, J. Bart, A.T. M. Willemsen, N.H. Hendrikse, Blood-brain barrier dysfunction in parkinsonian midbrain in vivo, Ann. Neurol. 57 (2005) 176–179, https://doi.org/10.1002/ana.20369.

[24] D.M.E. van Assema, M. Lubberink, M. Bauer, W.M. van der Flier, R.C. Schuit, A. D. Windhorst, E.F.I. Comans, N.J. Hoetjes, N. Tolboom, O. Langer, M. Müller, P. Scheltens, A.A. Lammertsma, B.N.M. van Berckel, Blood–brain barrier P-glycoprotein function in Alzheimer's disease, Brain. 135 (2012) 181–189, https://doi.org/10.1093/brain/awr298.

[25] M. Muzi, D.A. Mankoff, J.M. Link, S. Shoner, A.C. Collier, L. Sasongko, J. D. Unadkat, Imaging of cyclosporine inhibition of P-glycoprotein activity using 11C-verapamil in the brain: studies of healthy humans, J. Nucl. Med. 50 (2009) 1267–1275, https://doi.org/10.2967/jnumed.108.059162.

[26] M. Lubberink, Kinetic models for measuring P-glycoprotein function at the blood-brain barrier with positron emission tomography, Curr. Pharm. Des. 22 (2016) 5786–5792, https://doi.org/10.2174/1381612822666160804093852.

[27] M. Bauer, R. Karch, F. Neumann, A. Abrahim, C.C. Wagner, K. Kletter, M. Müller, M. Zeitlinger, O. Langer, Age dependency of cerebral P-gp function measured with (R)-[11C]verapamil and PET, Eur. J. Clin. Pharmacol. 65 (2009) 941–946, https://doi.org/10.1007/s00228-009-0709-5.

[28] F. Erdő, P. Krajcsi, Age-related functional and expressional changes in efflux pathways at the blood-brain barrier, Front. Aging Neurosci. 11 (2019) 1–8, https://doi.org/10.3389/fnagi.2019.00196.

[29] A.M.S. Hartz, A. Pekcec, E.L.B. Soldner, Y. Zhong, J. Schlichtiger, B. Bauer, P-gp protein expression and transport activity in rodent seizure models and human epilepsy, Mol. Pharm. 14 (2017) 999–1011, https://doi.org/10.1021/acs.molpharmaceut.6b00770.

[30] M. Bauer, R. Karch, M. Zeitlinger, J. Liu, M.J. Koepp, M.C. Asselin, S.M. Sisodiya, J. A. Hainfellner, W. Wadsak, M. Mitterhauser, M. Müller, E. Pataraia, O. Langer, In vivo P-glycoprotein function before and after epilepsy surgery, Neurology. 83 (2014) 1326–1331, https://doi.org/10.1212/WNL.0000000000000858.

[31] G. Pottier, S. Marie, S. Goutal, S. Auvity, M.-A. Peyronneau, S. Stute, R. Boisgard, F. Dolle, I. Buvat, F. Caille, N. Tournier, Imaging the impact of the P-glycoprotein (ABCB1) function on the brain kinetics of metoclopramide, J. Nucl. Med. 57 (2016) 309–314, https://doi.org/10.2967/jnumed.115.164350.

[32] H. Savolainen, A.D. Windhorst, P.H. Elsinga, M. Cantore, N.A. Colabufo, A. T. Willemsen, G. Luurtsema, Evaluation of [18F]MC225 as a PET radiotracer for measuring P-glycoprotein function at the blood-brain barrier in rats: kinetics, metabolism, and selectivity, J. Cereb. Blood Flow Metab. 37 (2017) 1286–1298, https://doi.org/10.1177/0271678X16654493.

[33] S. Auvity, F. Caillé, S. Marie, C. Wimberley, M. Bauer, O. Langer, I. Buvat, S. Goutal, N. Tournier, P-glycoprotein (ABCB1) inhibits the influx and increases the efflux of 11 C-metoclopramide across the blood-brain barrier: a PET study on non-human primates, J. Nucl. Med. (2018), https://doi.org/10.2967/jnumed.118.210104 jnumed.118.210104.

[34] N. Tournier, M. Bauer, V. Pichler, L. Nics, E.-M. Klebermass, K. Bamminger, P. Matzneller, M. Weber, R. Karch, F. Caillé, S. Auvity, S. Marie, W. Jäger, W. Wadsak, M. Hacker, M. Zeitlinger, O. Langer, Impact of P-glycoprotein function on the brain kinetics of the weak substrate 11 C-metoclopramide assessed with PET imaging in humans, J. Nucl. Med. 60 (2019) 985–991, https://doi.org/10.2967/jnumed.118.219972.

[35] L. García-Varela, W.M. Arif, D. Vállez García, T. Kakiuchi, H. Ohba, N. Harada, T. Tago, P.H. Elsinga, H. Tsukada, N.A. Colabufo, R.A.J.O. Dierckx, A. van Waarde, J. Toyohara, R. Boellaard, G. Luurtsema, Pharmacokinetic modeling of [18 F] MC225 for quantification of the P-Glycoprotein function at the blood–brain barrier in non-human primates with PET, Mol. Pharm. (2020), https://doi.org/10.1021/acs.molpharmaceut.0c00514 acs.molpharmaceut.0c00514.

[36] L. García-Varela, M. Rodríguez-Pérez, A. Custodia, R. Moraga-Amaro, N. A. Colabufo, P. Aguiar, T. Sobrino, R.A.J.O. Dierckx, A. van Waarde, P.H. Elsinga, G. Luurtsema, In vivo induction of P-glycoprotein function can be measured with [18 F]MC225 and PET, Mol. Pharm. (2021), https://doi.org/10.1021/acs.molpharmaceut.1c00302 acs.molpharmaceut.1c00302.

[37] P. Mossel, L. Garcia Varela, W.M. Arif, C.W.J. van der Weijden, H.H. Boersma, A.T. M. Willemsen, R. Boellaard, P.H. Elsinga, R.J.H. Borra, N.A. Colabufo, J. Toyohara, P.P. de Deyn, R.A.J.O. Dierckx, A.A. Lammertsma, A.L. Bartels, G. Luurtsema, Evaluation of P-glycoprotein function at the blood–brain barrier using [18F] MC225-PET, Eur. J. Nucl. Med. Mol. Imaging (2021) 10–11, https://doi.org/10.1007/s00259-021-05419-8.

[38] H. Savolainen, M. Cantore, N.A. Colabufo, P.H. Elsinga, A.D. Windhorst, G. Luurtsema, Synthesis and preclinical evaluation of three novel fluorine-18 labeled radiopharmaceuticals for P-glycoprotein PET imaging at the blood-brain barrier, Mol. Pharm. 12 (2015) 2265–2275, https://doi.org/10.1021/mp5008103.

[39] D.M.E. van Assema, M. Lubberink, R. Boellaard, R.C. Schuit, A.D. Windhorst, P. Scheltens, A.A. Lammertsma, B.N.M. van Berckel, P-glycoprotein function at the blood–brain barrier: effects of age and gender, Mol. Imaging Biol. 14 (2012) 771–776, https://doi.org/10.1007/s11307-012-0556-0.

[40] C. Kuntner, J.P. Bankstahl, M. Bankstahl, J. Stanek, T. Wanek, G. Stundner, R. Karch, R. Brauner, M. Meier, X. Ding, M. Müller, W. Löscher, O. Langer, Dose-response assessment of tariquidar and elacridar and regional quantification of P-glycoprotein inhibition at the rat blood-brain barrier using (R)-[11C]verapamil PET, Eur. J. Nucl. Med. Mol. Imaging 37 (2010) 942–953, https://doi.org/10.1007/s00259-009-1332-5.

[41] L. García-Varela, D. Vállez García, M. Rodríguez-Pérez, A. van Waarde, J.W. A. Sijbesma, A. Schildt, C. Kwizera, P. Aguiar, T. Sobrino, R.A.J.O. Dierckx, P. H. Elsinga, G. Luurtsema, Test–retest repeatability of [18 F]MC225-PET in rodents: a tracer for imaging of P-gp function, ACS Chem. Neurosci. 11 (2020) 648–658, https://doi.org/10.1021/acschemneuro.9b00682.

[42] D. Vállez Garcia, C. Casteels, A.J. Schwarz, R.A.J.O. Dierckx, M. Koole, J. Doorduin, A standardized method for the construction of tracer specific PET and SPECT rat brain templates: validation and implementation of a toolbox, PLoS One 10 (2015), e0122363, https://doi.org/10.1371/journal.pone.0122363.

[43] T. Wanek, K. Römermann, S. Mairinger, J. Stanek, M. Sauberer, T. Filip, A. Traxl, C. Kuntner, J. Pahnke, F. Bauer, T. Erker, W. Löscher, M. Müller, O. Langer, Factors governing P-glycoprotein-mediated drug-drug interactions at the blood-brain barrier measured with positron emission tomography, Mol. Pharm. 12 (2015) 3214–3225, https://doi.org/10.1021/acs.molpharmaceut.5b00168.

[44] L. Breuil, S. Marie, S. Goutal, S. Auvity, C. Truillet, W. Saba, O. Langer, F. Caillé, N. Tournier, Comparative vulnerability of PET radioligands to partial inhibition of P-glycoprotein at the blood-brain barrier: A criterion of choice? J. Cereb. Blood Flow Metab. (2021) https://doi.org/10.1177/0271678X211045444, 0271678X2110454.